Static Capacitance of Some Multilayered Microstrip Capacitors

Anand K. Verma, *Member, IEEE*, and Zargham Rostamy

***Abstract*—A new unified model, the modified Wolff model (MWM) is presented to determine the lumped capacitance of rectangular, circular, hexagonal and triangular patches on the single layer substrate and under the multilayer condition. Effect of the top shield on the lumped capacitance has also been determined. The MWM is the combination of Wolff-Knoppick model, TTL technique and single layer reduction (SLR) technique. The results of MWM have been compared against the results of SDA, FEM, dual integral method and other forms of the variational methods with accuracy between 0.5–5% for the most of shapes under various conditions. The present model has accuracy of SDA and other rigorous formulations. No single method has been used in the literature to determine the lumped capacitance of patches of several shapes under the multilayer and shielded condition. The MWM is fast even on the desktop computer. Thus, the model is suitable for a unified CAD for the MMIC applications.**

I. Introduction

THE increasing use of integrated circuits at microwave frequencies has created a great deal of interest in the theoretical study of static capacitance of the microstrip patches of various shapes like rectangle, circle, hexagon, triangle, etc. Such lumped capacitor elements are integrated to realize the desired functional devices. For the MMIC technology, these lumped static capacitances must be determined under the multidielectric layers condition. However, most of the analytical results of such patch capacitors have been reported on the single layer substrate. Even for the single layer substrate, a single method has not been applied to determine capacitance of the patches of various shapes.

The lumped capacitance of rectangular patch has been determined by Farrar and Adams [1], Itoh *et al.* [2], Benedek and Silvester [20], and Wolff and Knoppik [3] using the point matching technique, the SDA, the integral equation method and the transmission line method respectively. The first method suffers from large matrix inversion. The SDA is also not very efficient for the CAD application and its results for the multilayer patch is not available. Wolff and Knoppik model has deviation more than 30% against the Benedek and Silvester for $2h/W \geq 1$ i.e., for the narrow line. Bedair [4] has improved the results by including the corner capacitance.

The lumped capacitance of a microstrip circular patch has been determined by Itoh and Mitra using the SDA with Hankel transform [5], by Borkar and Yang [6], Leong *et al.* [7], [8] and Chew and Kong [9] using the dual integral formulation, and by Wolff and Knoppik 2 [3] treating the circular patch as a deformed rectangular patch. The SDA results of Itoh and Mitra are within 3% against the experimental results at 1.542 MHz for $\epsilon r = 2.65$.

Using the static SDA method, the lumped capacitance of hexagonal and triangular microstrip patches have been obtained by Sharma and Hoefer [10]. However, the calculated resonance frequency of the hexagonal patch based upon such calculated capacitance shows deviation more than 2% from the experimental results.

None of the above discussed methods has been used to obtain either the lumped capacitance of the shielded patch or the lumped capacitance of the multidielectric microstrip patch. Moreover, a single method except the SDA, has not been used to calculate the lumped capacitance of microstrip patch of various shapes. Leong *et al.* [11] have used the finite element method (FEM) to calculate the lumped capacitance of a shielded circular microstrip disk. However, the FEM results do not converge easily. Bhat and Koul [12] have used the double Fourier integral (DFI) method to determine the lumped capacitance of rectangular suspended, inverted and sandwiched patches. Accurate numerical evaluation of the double Fourier integral (DFI) is difficult and the method of its evaluation has not been discussed by the authors.

In this paper, the model of Wolff and Knoppik [3] has been modified with the help of the transverse transmission line (TTL) technique [13] to compute the lumped capacitance of the shielded and multilayer microstrip patches having rectangular, circular, hexagonal and triangular shapes. The calculated results, using the modified Wolff model (MWM) show good agreement with the available numerical results. The modified Wolff model [14], [15] has already been used successfully with accuracy of about 0.5% to determine the resonance frequency of the microstrip patches with and without dielectric cover. However, capacitance of the narrow rectangular patch and small circular disk has not been discussed previously.

II. Formulation of the MWM to Determine Lumped Capacitance

The four-layered shielded microstrip patch is shown in Fig. 1. In the Modified Wolff Model (MWM) total capacitance of the disk is the summation of the central capacitance of the patch, the fringe capacitance along the boundary and the corner capacitance under the multidielectric layer condition. We have assumed that the central capacitance of the patch is not influenced by the presence of top shield and the dielectric superstrate as they influence only the fringe field not the

Manuscript received June 1, 1993; revised September 2, 1994.

The authors are with the Department of Electronics Science, University of Delhi, New Delhi 110021, India.

IEEE Log Number 9410340.

permittivity of the substrate material. The assumption has been confirmed by the accurate determination of resonance frequency of the dielectric covered microstrip patch [14], [15]. Thus, the total lumped capacitance of the multilayered rectangular patch is given by

$$\begin{aligned} C_T(\epsilon r_1 \cdots \epsilon r_4, W, L, h_1 \cdots h_4) &= C_o(\epsilon r_1, \epsilon r_2, W, L, h_1, h_2) \\ &+ 2C_{e1}(\epsilon r_1 \cdots \epsilon r_4, W, L, h_1 \cdots h_4) \\ &+ 2C_{e2}(\epsilon r_1 \cdots \epsilon r_4, W, L, h_1 \cdots h_4) \\ &+ 4C_c(\epsilon r_1 \cdots \epsilon r_4, W, L, h_1 \cdots h_4) \end{aligned} \quad (1)$$

where, C_o is the central capacitance, which depends upon permittivity and height of dielectric layers between the patch and ground plane. C_{e1} and C_{e2} are the static fringe capacitances along one side of length L and width W, respectively. C_c is the corner capacitance. These capacitances could be calculated as follows:

$$C_o(\epsilon r_1, \epsilon r_2, W, h_1, h_2) = \frac{\epsilon_o \epsilon_{eq} A}{h} \quad (2)$$

where, ϵ_{eq} is the equivalent permittivity of the composite substrate. For the two layers substrate, it could be obtained form the results of Dahele and Lee [16], given below

$$\epsilon_{eq} = \frac{\epsilon r_1 \epsilon r_2 (h_1 + h_2)}{\epsilon r_1 h_2 + \epsilon r_2 h_1}. \quad (3)$$

However, this method does not account for the effect of width on the equivalent permittivity. The equivalent permittivity for the composite substrate of two or more dielectric layers could also be obtained by the single layer reduction (SLR) techniques developed by Verma *et al.* [17]. The SLR technique has been followed in this paper, as it gives more accurate ϵ_{eq} which depends upon width of the patch. $h = h_1 + h_2$ is total height of the composite structure. A is area of the patch.

The fringe capacitance is obtained from the following expression [15]:

$$C_{e1}(\epsilon r_1 \cdots \epsilon r_4, W, L, h_1 \cdots h_4) = \frac{1}{2}\left[\frac{Z_o(W, h_1 \cdots h_4, \epsilon r_1 \cdots \epsilon r_4 = 1)L}{V_o Z^2(W, h_1 \cdots h_4, \epsilon r_1 \cdots \epsilon r_4)} - \frac{\epsilon_o \epsilon_{eq} A}{h}\right]. \quad (4)$$

$Z_o(\epsilon r_1 = \cdots \epsilon r_4 = 1, W, h_1 \cdots h_4)$ and $Z(\epsilon r_1 \cdots \epsilon r_4, W, h_1 \cdots h_4)$ are the characteristic impedances of the patch of width W on the air-substrate and the multilayered dielectric substrate respectively. V_o is the velocity of light. The characteristic impedance can be calculated by using the variational method along with TTL technique to obtain the Green's function of the structure. The capacitance per length of a line is obtained from

$$\frac{1}{C} = \frac{1}{\pi \epsilon_o} \int_o^\infty \frac{\left[\frac{f(\beta)}{Q}\right]^2}{\beta} \frac{1}{Y} d\beta \quad (5)$$

where, Q is the total charge on the conducting patch and $f(\beta)$ is the Fourier transform of the charge distribution function.

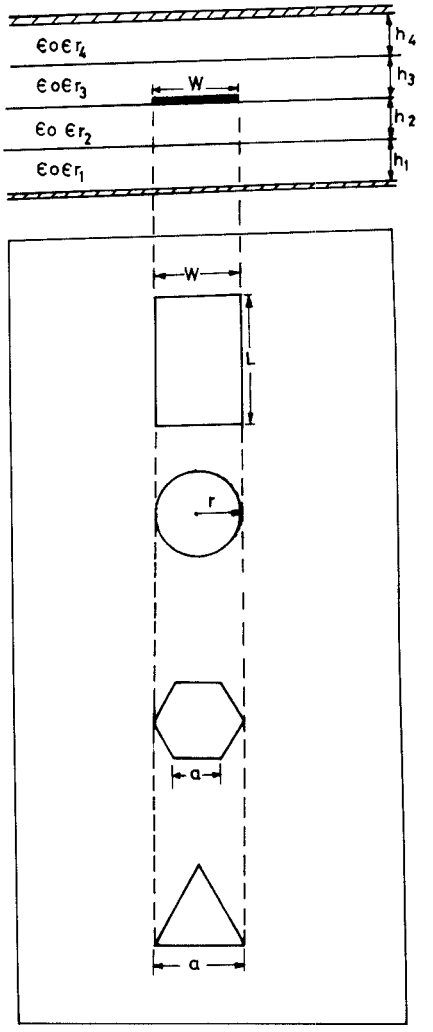

Fig. 1. Geometrically different four layers shielded structure.

The charge distribution function of Yamashita [18] has been taken in the present formulation. Y, the admittance function signifying the Green's function of the problem is obtained from the TTL technique [13]. Green's function is independent of shape of the patch. For a four layers structure Y is given by the following expression:

$$Y = \epsilon r_2 \left[\frac{\epsilon r_1 \coth(\beta h_1) + \epsilon r_2 \tanh(\beta h_2)}{\epsilon r_2 + \epsilon r_1 \coth(\beta h_1) \tanh(\beta h_2)}\right] + \epsilon r_3 \left[\frac{\epsilon r_4 \coth(\beta h_4) + \epsilon r_3 \tanh(\beta h_3)}{\epsilon r_3 + \epsilon r_4 \tanh(\beta h_3) \coth(\beta h_4)}\right]. \quad (6)$$

The effective dielectric constant and the characteristic impedance of the multilayer microstrip line could be obtained from the following expressions:

$$\epsilon_{eff}(W) = \frac{C}{C_o} \quad (7)$$

and

$$Z(\epsilon r_1 \cdots \epsilon r_4, W, h_1 \cdots h_4) = \frac{1}{V_o \sqrt{\frac{C}{C_o}}} \quad (8)$$

TABLE I
DETERMINATION OF CHARACTERISTIC IMPEDANCE IN OHMS

W/h1	I [23]	II (Eq.8)	III (Eq.9)	%. Error		I [23]	II (Eq.8)	II (Eq.9)	% Error	
				II	III				II	III
	$\epsilon_{r1} = 2.1$					$\epsilon_{r1} = 11.9$				
0.05	239.79	199.03	238.66	16.99	0.47	115.17	95.14	114.10	17.39	0.93
0.10	206.79	192.25	206.01	6.89	0.23	98.81	91.83	98.32	7.06	0.49
1.00	96.41	98.6	96.80	2.27	0.03	45.04	45.76	45.07	1.59	0.07
5.00	36.41	36.44	36.66	0.77	0.00	16.07	16.17	16.05	0.62	0.12
10.0	20.78	18.40	21.05	11.45	1.30	9.09	7.91	8.87	12.96	2.42

Where C and C_o are respectively the capacitances per unit length of line with dielectrics and all dielectrics replaced by the air. V_o is the velocity of light.

The characteristic impedance of the multilayer microstrip line can also be determined from the following expression:

$$Z(\epsilon r_1 \cdots \epsilon r_4, W, h_1 \cdots h_4) = \frac{Z_o(\epsilon r_1 \cdots \epsilon_4 = 1, W, h_1 \cdots h_4)}{\sqrt{\epsilon_{eff}(W)}}. \quad (9)$$

Where $Z_o(\epsilon r_1 \cdots \epsilon r_4 = 1, W, h_1 \cdots h_4)$ is the characteristic impedance of the microstrip line on the air substrate. It could be determined accurately by the closed form expressions of either Hammerstad-Jensen or Schneider or Wheeler as summarized by Hoffman [23]. Table I shows that the calculated characteristic impedance from (8) and (9) compared against the results of methods of line summarized by Hoffman, has average accuracy of 8.8% and 0.6%, respectively for the microstrip line on $\epsilon r_1 = 2.1$, 11.9 in the range $0.5 \leq W/h_1 \leq 10$. The closed form expression of Hammerstad-Jansen for the characteristic impedance of the microstrip line on air substrate and the variational expression to determine ϵ_{eff} of the multilayer microstrip line have been used in (9). Gauss-Lagauree integration scheme has been used to evaluate the variational integral (5). Thus, due to its better numerical accuracy expression (9) is recommended for the CAD application.

Likewise, $C_{e2}(\epsilon r_1 \cdots \epsilon r_4, L, h_1 \cdots h_1)$ can be calculated by exchanging W for L and L for W in (4).

The corner capacitance of a rectangular microstrip patch has been obtained by Bedair [4]. His result can be modified as follows for the rectangular patch under the multilayer conditions:

$$C_c(\epsilon r_1 \cdots \epsilon r_4, W, L, h_1 \cdots h_4) = \left[\frac{(W_{eq} - W)C_{e2}(\epsilon r_1 \cdots \epsilon r_4, L, h_1 \cdots h_4)}{W} + \frac{(L_{eq} - L)C_{e1}(\epsilon r_1 \cdots \epsilon r_4, W, h_1 \cdots h_4)}{L}\right] \Big/ 32 \quad (10)$$

where C_{e1} and C_{e2} can be obtained from (4).

The equivalent width W_{eq} and equivalent length L_{eq} can be obtained from the planar waveguide model of the microstrip [19]. The planar waveguide model could also be adopted for the multilayered microstrip patch as follows:

$$W_{eq} = \frac{120\pi h}{Z(\epsilon r_1 \cdots \epsilon r_4, W, h_1 \cdots h_4)\sqrt{\epsilon_{eff}(W)}}. \quad (11)$$

Likewise, L_{eq} can also be calculated. However, Bedair [4] has calculated W_{eq} for the air substrate without taking into account permittivity of the substrate.

A. Microstrip Rectangular Patch

The four layers structure could be reduced to many useful structures by changing the values of $h_1 \cdots h_4$ and $\epsilon r_1 \cdots \epsilon r_4$.

The structure of Fig. 1 can be reduced to a microstrip patch by taking $h_4 \to \infty$, $h_2 \to 0$, $h_3 \to 0$, $\epsilon r_4 = 1$. The admittance function from (6) for this structure is given by

$$Y = 1 + \epsilon r_1 \coth(\beta h_1). \quad (12)$$

The normalized lumped capacitance of the microstrip patch calculated by the MWM for square patch on $\epsilon r_1 = 1$ and $\epsilon r_1 = 9.6$ is shown in Fig. 2. Normalization has been done by the central capacitance given by (2). Fig. 2 also presents results of Itoh *et al.* [2]. For $h_1/W \leq 1$, the two methods show excellent agreement. However, for $h_1/W > 1$ the results of MWM are a little higher than the results of SDA. Maximum deviation in results for $h_1/W = 10$ i.e., for a very narrow patch is 4%. Fig. 3 shows the normalized capacitance of the rectangular patch on $\epsilon r_1 = 1$ for various aspect ratios calculated by the MWM, Bedair [4] and Benedek and Silvester [20]. Effect of the corner capacitance on the lumped capacitance is significant for $2h_1/W = 10$, by including the corner capacitance deviation in the results of MWM against Bendek and Silvestar improves from 30–8%. For the wider patch, effect of the corner capacitance is not significant. In the case of microstrip patch, the MWM formulation reduces to the formulation of Bedair, however with a small change due to our accounting of the permittivity of the substrate for calculating W_{eq} which has been neglected by Bedair.

B. Microstrip Circular Patch

The MWM has been used to calculate accurately the lumped capacitance of a circular patch. The admittance function given by (6) is also applicable to microstrip circular patch. The total capacitance of circular patch is given by the following expression:

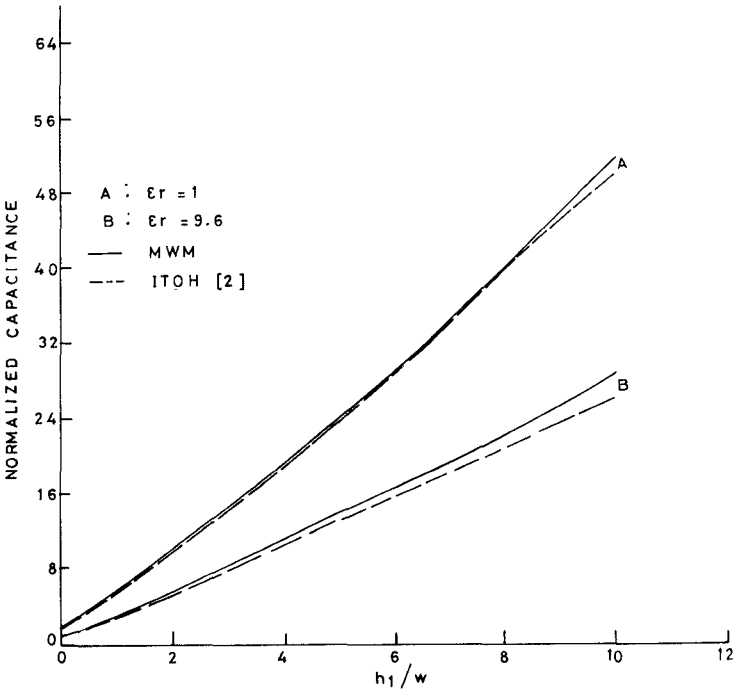

Fig. 2. Normalized capacitance of the square patch. x axis: patch width h_1/w; y axis: normalized capacitance.

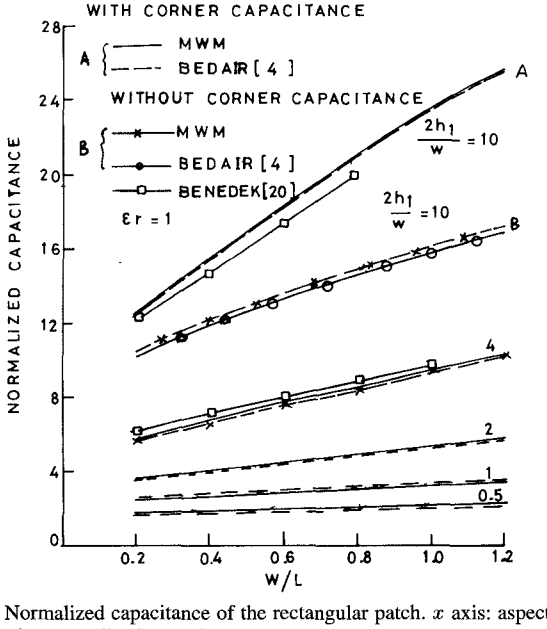

Fig. 3. Normalized capacitance of the rectangular patch. x axis: aspect ratio w/l; y axis: normalized capacitance.

$$C_T(\epsilon r_1 \cdots \epsilon r_4, 2r_o, h_1 \cdots h_4) = C_o(\epsilon r_1, \epsilon r_2, 2r_o, h_1, h_2) + C_e(\epsilon r_1 \cdots \epsilon r_4, W = 2r_o, h_1 \cdots h_4) + 2C_c(\epsilon r_1 \cdots \epsilon r_4, 2r_o, h_1 \cdots h_4) \quad (13)$$

where C_o is the central capacitance given by (2) with $A = \pi r_o^2$. C_e is the fringe capacitance calculated by transforming the circular patch into an equivalent rectangular patch of width $W = 2r_o$. Wolff and Knoppik have taken length of the equivalent rectangular patch $L = \pi r_o$ whereas, Bedair has taken $L = 2\pi r_o$. By maintaining the invariance of the electrostatic energy below the patch we have taken $L = \pi r_o/2$ for the circular patch. Thus, the fringe capacitance is obtained from

$$C_e(\epsilon r_1 \cdots \epsilon r_4, W = 2r_o, h_1 \cdots h_4) = 2C_{e1}(\epsilon r_1 \cdots \epsilon r_4, W = 2r_o, h_1 \cdots h_4) \quad (14)$$

where C_e1 is obtained from (4).

The fringe fields of original circular patch and the deformed rectangular patch are not identical. However, by considering two corner capacitances at the opposite end of the diameter which forms width of the deformed rectangular patch fringe field of the original circular patch could be modeled more accurately. The corner capacitance has not been added to the circle, it is added in the equivalent deformed rectangle. The corner capacitance C_c for the deformed rectangular patch can be calculated by (10). Bedair has not taken into account the corner capacitance in the deformed rectangular patch while determining the lumped capacitance of a circular patch.

The lumped capacitances of a circular microstrip disk on $\epsilon r_1 = 1$, 2.65, and 9.6 calculated by the Noble's variational method [8], Bedair [4], Chew and Kong [9], the SDA [5] using both the Gate and Maxwell charge distribution functions and the MWM are shown in Table II. Results obtained by the MWM with two corner capacitance and without corner capacitance have also been shown in Table II. Taking the Noble's variational method [8] as reference, the Table III(a) shows analysis of deviation of lumped capacitance calculated by various methods for $\epsilon r_1 = 1$. The SDA results with the Maxwell's distribution function shows the best agreement. Results of Bedair and Chew and Kong shows progressive increase in the deviation with increase in h_1/r_o ratio from

TABLE II
COMPARISON OF VARIOUS METHODS TO DETERMINE NORMALIZED LUMPED CAPACITANCE OF A CIRCULAR DISK (NORMALIZATION W R T. CENTRAL CAPACITANCE)

* MWM results with corner capacitance

\+ MWM reslut witout corner capacitance

ϵr	h/r_o	Variational [8]	Bedair [4]	Kong [9]	SDA [5] Gate	SDA [5] Maxwell	MWM*	MWM+
1	0.1	1.3159	1.342	1.32	1.2553	1.4072	1.3411	1.342
	0.5	2.3179	2.260	2.32	2.1075	2.3630	2.3001	2.257
	1.0	3.5343	3.211	3.81	3.2095	3.3524	3.3001	3.211
	5.0	13.592	-	-	12.514	13.592	12.016	9.665
	10.0	26.300	-	-	24.270	26.300	24.191	16.49
2.65	0.1	1.1780	1.190	1.18	1.1363	1.2663	1.2064	1.200
	0.5	1.8094	1.753	1.80	1.6463	1.8379	1.8084	1.780
	1.0	2.6121	2.399	2.72	2.3644	2.6309	2.5266	2.436
	5.0	9.4866	-	-	8.7256	9.4874	8.8261	6.887
	10.0	18.231	-	-	16.189	18.231	16.912	11.61
9.6	0.1	1.1124	1.123	1.11	1.08	1.1972	1.1470	1.148
	0.5	1.5749	1.530	1.58	1.4347	1.6255	1.5920	1.578
	1.0	2.1942	2.041	2.25	1.9824	2.2132	2.1610	2.090
	5.0	7.6718	-	-	7.0516	7.6725	6.9951	6.706
	10.0	14.677	-	-	13.536	14.677	13.716	9.499

TABLE III
(a) ANALYSIS OF % DEVIATION IN NORMALIZED LUMPED CAPACITANCE OF CIRCULAR PATCH W. R. t VARIATIONAL METHOD [8] (NORMALIZATION W R T CENTRAL CAPACITANCE (b) % RMS DEVIATION IN NORMALIZED LUMPED CAPACITANCE CALCULATED BY VARIOUS METHODS

* MWM results with corner capacitance

\+ MWM results without corner capacitance

$\epsilon r_1 = 1$

h_1/r_o	Bedair[4] %	Kong [9] %	SDA,Gate % [5]	[5] Maxwell%	MWM* %	MWM+ %
0.1	-1.98	-0.31	+4.6	-6.94	- 1.95%	-1.83
0.3	-0.34	-0.60	+8.0	-3.69	- 1.13%	-0.17
0.5	+2.50	-0.09	+9.1	-1.95	+0.76	+2.63
0.7	+5.32	-2.74	+9.3	-1.1	+2.61	-1.70
0.9	+7.88	-5.80	+9.26	-0.65	+4.22	+8.00
1.0	+9.15	7.8	+9.19	-0.51	+4.92	+9.15
3.0	-	-	+8.23	-0.03	+11.21	+23.01
5.0	-	-	+7.93	-0.00	+11.59	+23.01
7.0	-	-	+7.80	-0.03	+10.57	+29.01
9.0	-	-	-17.72	-0.00	+8.94	+36.30
10.0	-	-	-17.72	-0.00	+8.02	+37.50

(a)

TABLE III
(Continued)

h_1/r_o	ϵr_1	Bedair [4] %	Kong [9] %	Gate %	Maxwell %	MWM* %	MWM+ %
0.1-1.0	1.00	5.54	4.14	8.41	3.35	3.00	5.18
1-10	1.00	-	-	8.18	2.48	7.20	22.13
0.1-1.0	2.65	5.12	2.15	8.34	3.87	2.17	3.99
1-10	2.65	-	-	8.24	4.08	5.78	21.06
01-1.0	9.60	3.98	1.17	8.31	4.16	1.79	2.99
1-10	9.60	-	-	8.18	3.07	5.45	19.96

(b)

0.1 to 1. The deviation in results of Bedair increases from 1.98–9.15%. Whereas, the deviation in the results of Chew and Kong increases form 0.31–7.8%. The MWM results without corner capacitance is almost identical with the results of Bedair, giving deviation 1.83 and 9.15% for $h_1/r_o = 0.1$ and 1, respectively. For $1 \leq h_1/r_o \leq 10$ without the corner capacitance, the deviation calculated by the MWM increases from 9.15–37.5%. Same would have been results from the method of Bedair. However, with two corners capacitance included maximum deviation in the results calculated by the MWM is only 11.59%. The Table III(b) shows the rms deviation of various methods. It is obvious that the deviation decreases with increase in the permittivity of the substrate. This behavior is due to concentration of more field below the patch. For $0.1 \leq h_1/r_o \leq 1$ the deviation in results calculated by the MWM which includes corner capacitance is 3%, 2.17%, and 1.79% for $\epsilon r_1 = 1$, 2.65, and 9.6, respectively. However, in the range $1 \leq h_1/r_o \leq 10$, the deviation is 7.2%, 5.78%, and 5.45% for $\epsilon r_1 = 1$, 2.65, and 9.6, respectively. Thus, the results obtained by the MWM for the lumped capacitance of the circular disc are accurate for the wide range of h_1/r_o ratios and the permittivities.

C. Microstrip Hexagonal and Triangular Patches

The MWM can be used to determine the capacitance of hexagonal and triangular patches by converting these to an

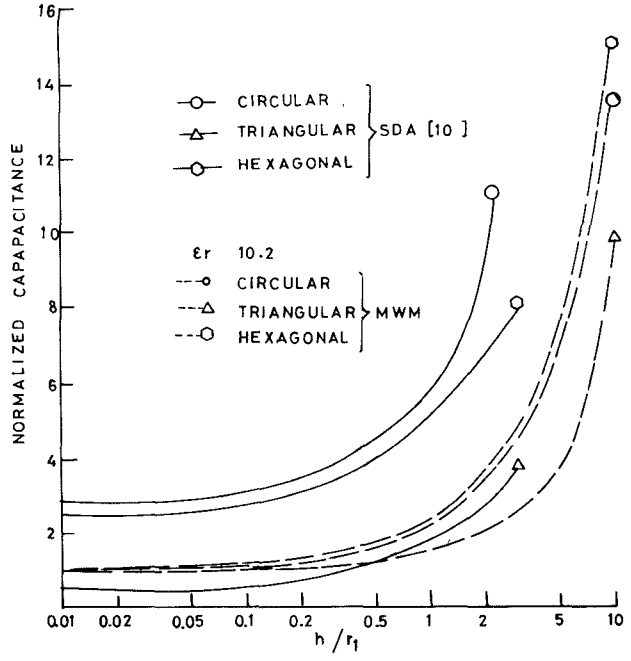

Fig. 4. Normalized capacitance of the circular triangular and hexagonal patches. x axis: h/r_1; y axis: normalized capacitance.

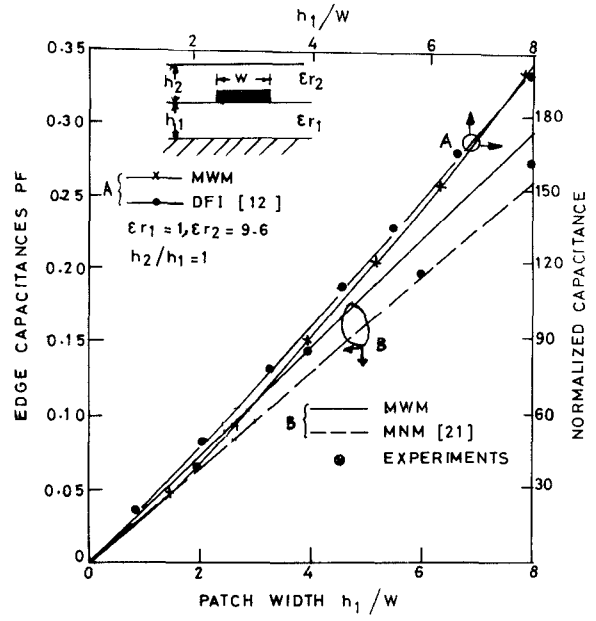

Fig. 5. Edge capacitance of the dielectric covered rectangular patch and normalized capacitance of square inverted rectangular patch. x axis: patch width h_1/w; y axis: edge capacitance Pf.

equivalent circular patch. Fig. 4 shows the results of normalized static capacitance of circular, hexagonal and triangular patches computed by the MWM and the results are compared against the SDA results of Sharma and Hoefer [10]. The results of normalized capacitance of the circular patch obtained by the SDA are higher than that of the results obtained by MWM. However, the results of resonance frequency of circular patch calculated by the MWM give deviation within 0.5% against the experimental resonance frequency and against the resonance frequency calculated by various full wave method [15]. Likewise, resonance frequency of the hexagonal patch calculated by the MWM is more accurate than that of resonance frequency calculated by Sharma and Hoefer [22]. Thus, the lumped capacitances of the circular and hexagonal patches calculated by the MWM are more accurate. For $h_1/r_o \leq 3$, the lumped capacitance of the triangular patch obtained by the MWM follows closely the results of Sharma and Hoefer. The inaccuracy in the results of SDA is due to the convergence problem associated with the infinite integrals involved in the formulation of the SDA.

III. Lumped Capacitance of Dielectric Covered Patch

The MWM has already been used to determine the resonance frequency of dielectric covered rectangular and circular patch with accuracy of 0.5% [14], [15]. The theory presented in the previous section can be used to calculate the lumped capacitance of the rectangular (square), circular, hexagonal and triangular patches alongwith the dielectric superstrate. Even a thin layer of the superstrate has much influence on the lumped capacitance of the patch. The admittance function of the dielectric covered microstrip structure obtained from (6) is given by

$$Y = \epsilon r_1 \coth(\beta h_1) + \epsilon r_3 \left[\frac{\epsilon r_3 + \coth(\beta h_3)}{1 + \epsilon r_3 \coth(\beta h_3)}\right] \tag{15}$$

Fig. 5 for $h_3 = h_2$, $\epsilon r_3 = \epsilon r_2$ shows the edge capacitance of the covered rectangular patch for $\epsilon r_1 = \epsilon r_2 = 2.6$ and $h_2/h_1 = 6.25$ obtained by the MWM and by Benalla and Gupta [21]. However, Benalla and Gupta have not considered the corner capacitances. Therefore, the calculated value of edge capacitance by them is lower than that of values obtained by the MWM. The inverted patch is a special case of the dielectric covered microstrip patch. Fig. 5 also compares the calculated normalized capacitance of the square inverted patch obtained by the MWM and the double Fourier integral (DFI) method. For $\epsilon r_1 = 9.6$, $h_2/h_1 = 1$, results show excellence agreement. Figs. 6–9 show the effect of superstrate on the normalized lumped capacitance of the square, circular, hexagonal, and triangular patches. The influence of the superstrate is maximum on normalized lumped capacitance of the square patch and minimum on the triangular patch. Moreover, the superstrate of high permittivity material has more influence, as more field lines move toward the superstrate. Fig. 10 shows the comparison of normalized capacitance of circular patch for the inverted and suspended structures. For the same h_2/h_1 ratio, both of them provide with nearly same lumped capacitance. The suspended structure has slightly higher value of the normalized lumped capacitance.

IV. Lumped Capacitance of Patch on a Composite Substrate

The admittance function for two layers composite structure obtained from (6) is given by

$$Y = 1 + \epsilon r_2 \left[\frac{\epsilon r_1 \coth(\beta h_1) + \epsilon r_2 \tanh(\beta h_2)}{\epsilon r_2 + \epsilon r_1 \coth(\coth(\beta h_1) \tanh(\beta h_2)}\right]. \tag{16}$$

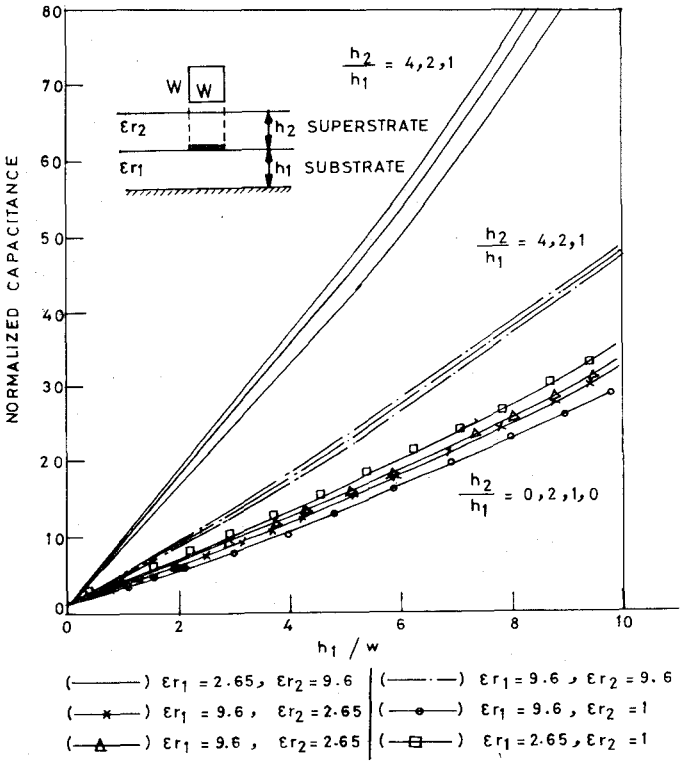

Fig. 6. Effect of cover on lumped capacitance of square patch. x axis: patch width h_1/w; y axis: normalized capacitance.

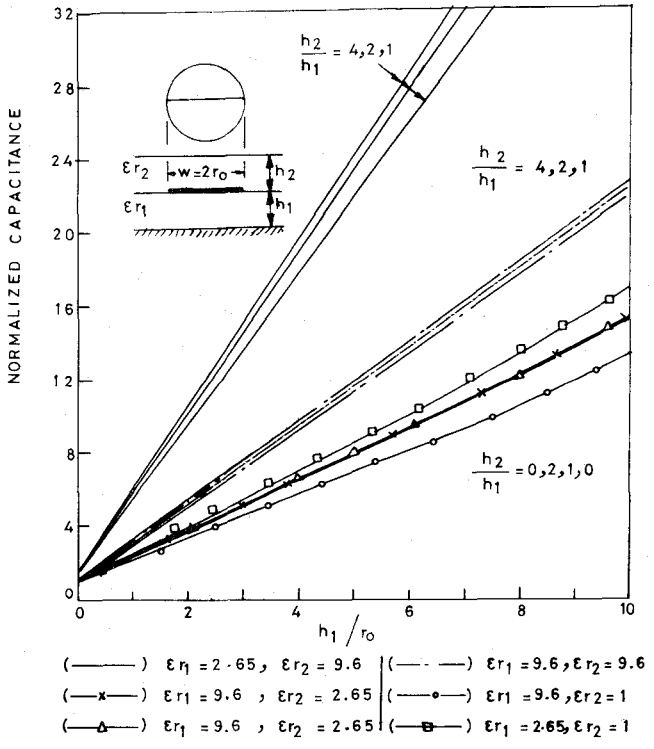

Fig. 7. Effect of cover on lumped capacitances of circular disk. x axis: patch radius h_1/r_o; y axis: normalized capacitance.

Fig. 11 shows the normalized lumped capacitance of a rectangular patch capacitor on the GaAs ($\epsilon r_1 = 12.95$) with the passivation layer of polyimide ($\epsilon r_2 = 3.5$). Even a thin passivation layer significantly influences the lumped capacitance.

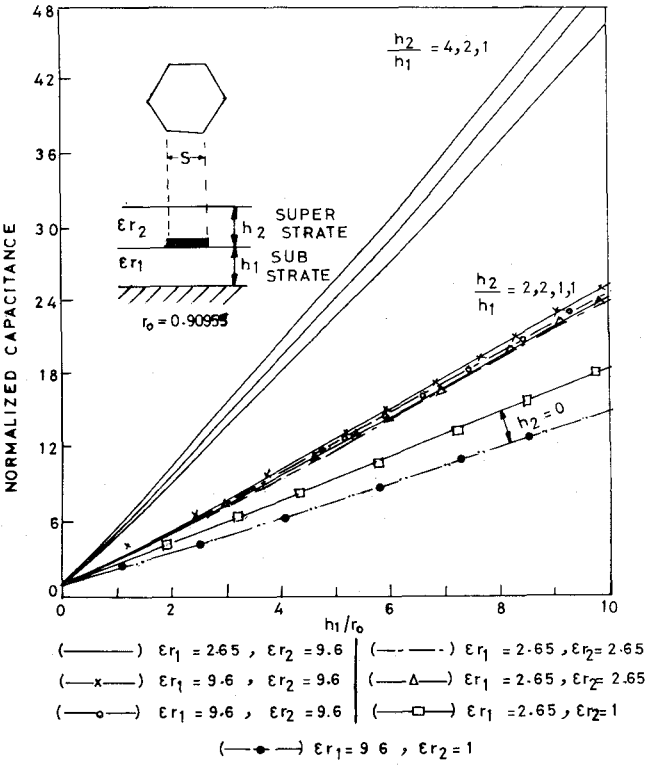

Fig. 8. Effect of cover on lumped capacitances of hexagonal patch. x axis: patch radius h_1/r_o; y axis: normalized capacitance.

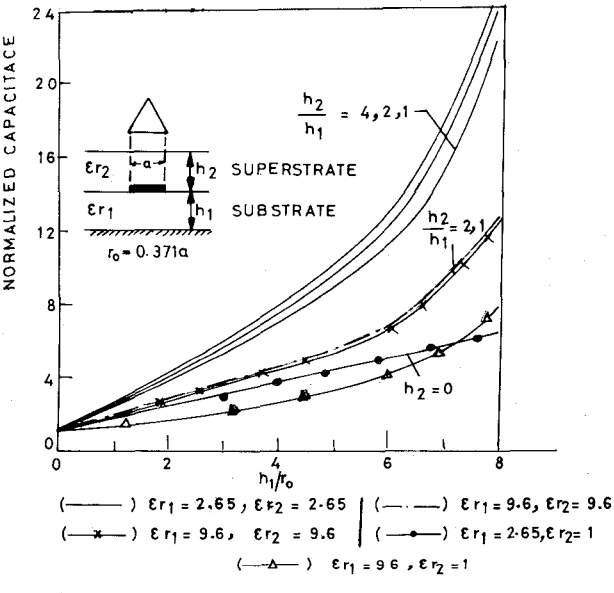

Fig. 9. Effect of cover on lumped capacitances of triangular patch. x axis: patch radius h_1/r_o; y axis: normalized capacitance.

V. Lumped Capacitance of a Shielded Patch

Effect of the shield on the lumped capacitance of a microstrip patch can be also treated with help of the MWM. The four layers shielded structure can be reduced to the shielded microstrip patch whose admittance function is given by

$$Y = \epsilon r_1 \coth(\beta h_1) + \coth(\beta h_2) \tag{17}$$

where, h_2 is height of the shield.

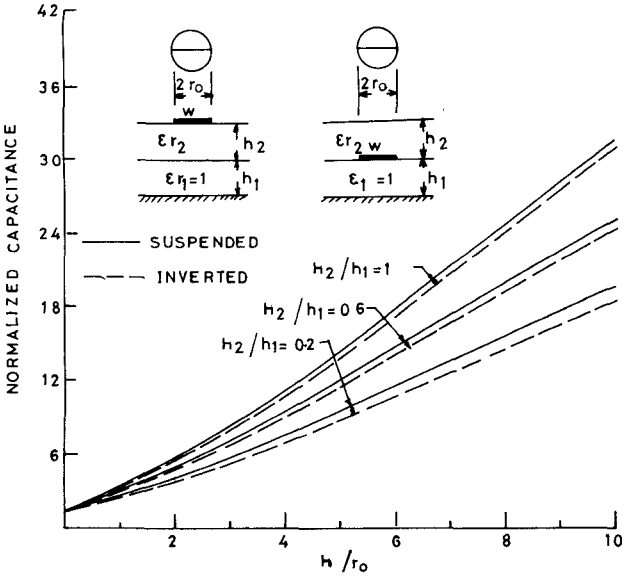

Fig. 10. Normalized capacitance of circular suspended and inverted structure. x axis: patch radius h/r_o; y axis: normalized capacitance.

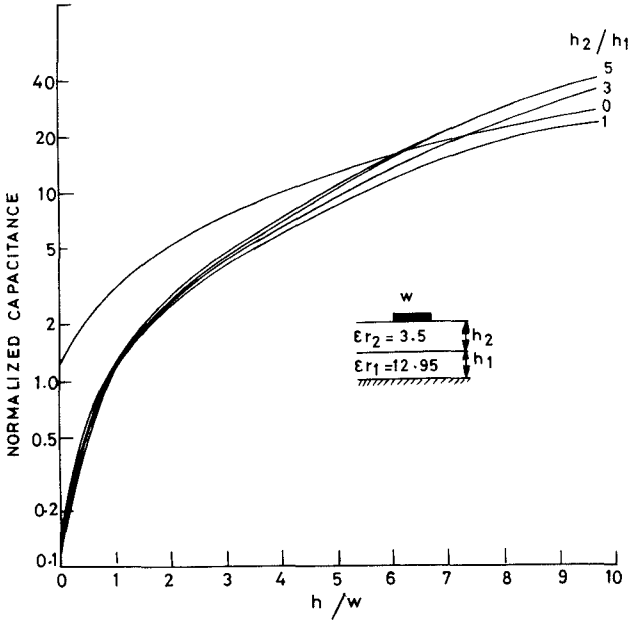

Fig. 11. Lumped capacitance of composite substrate. x axis: patch radius h/w; y axis: normalized capacitance.

The lumped capacitance of a shield microstrip circular patch has been obtained by Leong *et al.* [11] using the finite element method (FEM). They have taken the patch on $\epsilon r_1 = 1$, 2.65, and 9.6, and h_1/r_o varying from 0.1–1.0. Table IV shows the normalized capacitance of the shielded circular patch calculated by the FEM and MWM. Presence of the top shield increases the normalized capacitance. Normalization has been done by $\epsilon r_1 \pi r_o^2/h_1$, where r_o is radius of the patch. For the high permittivity substrate, the results obtained from the MWM are a little greater than the results of FEM. The deviation is more for the patch on the air substrate. On the dielectric substrate $\epsilon r_1 = 2.65$ and 9.6 deviation is between 0.2% to 6% for $0.1 \leq h_1/r_o \leq 1$. For $\epsilon r_1 > 9.6$ and $h_1/r_o \leq 1$ deviation decreases.

TABLE IV
NORMALIZED CAPACITANCE OF A SHIELD CIRCULAR PATCH (NORMALIZATION W.R.T. CENTRAL CAPACITANCE)

ϵr_1	h_1/r_o	$h_2 = r_o$ Leong [11]	MWM	$h_2 = 2r_o$ Leong [11]	MWM
1.00	0.1	1.341	1.434	1.326	1.367
	0.5	2.519	2.899	2.324	2.478
	1.0	4.047	4.726	2.621	2.781
2.65	0.1	1.191	1.241	1.185	1.216
	0.5	1.883	2.009	1.812	1.857
	1.0	2.790	2.977	2.630	2.625
9.6	0.1	1.121	1.157	1.118	1.510
	0.5	1.604	1.637	1.582	1.596
	1.0	2.279	2.241	2.194	2.144

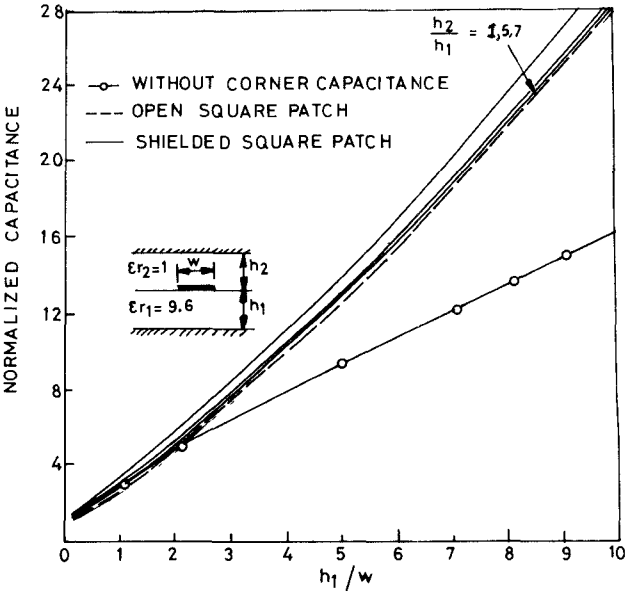

Fig. 12. Normalized capacitance of shielded square patch.x axis: patch radius h_1/w; y axis: normalized capacitance.

Fig. 12 shows the effect of shield on the lumped capacitance of a square patch made on the substrate $\epsilon r_1 = 9.6$. The effect of the shield is more pronounced on the smaller patch i.e., for $h_1/W > 2$. For the shield height $h_2/h_1 \geq 7$, effect of the shield on the lumped capacitance can be ignored.

VI. CONCLUSION

The modified Wolff model (MWM) is an efficient CAD tool for the determination of the lumped capacitance of patches of several shapes under the multilayer condition. The effect of the shield on the lumped capacitance has also been taken into account. Accuracy of the model has been verified against the available theoretical formulations. No other method has been used to determine the lumped capacitance of microstrip patches for various shapes under multilayer conditions for the MMIC applications.

ACKNOWLEDGMENT

The authors would like to thank unknown reviewers for suggesting improvement in the manuscript. The first author expresses his gratitude to Dr. Enakshi K Sharma for taking interest in this work.

REFERENCES

[1] A. Farrar and A. T. Adams, "Computation of lumped microstrip capacities by matrix methods. Rectangular sections and end effects," *IEEE Trans. Microwave Theory Tech.*, vol. MTT-9, pp. 495–497, May 1971; also "Correction," *IEEE Trans. Microwave Theory Tech.*, vol. MTT-20, p. 294, Apr. 1972.

[2] T. Itoh, R. Mitra, and R. D. Ward, "A method for computing edge capacitance of finite and semi-infinite microstrip lines," *IEEE Trans. Microwave Theory Tech.*, vol. MTT-20, pp. 847–849, Dec. 1972.

[3] I. Wolff and N. Knoppik, "Rectangular and circular microstrip disk capacitors and resonators," *IEEE Trans. Microwave Theory Tech.*, vol. MTT-22, pp. 857–864, 1974.

[4] S. S. Bedair, "Closed from expressions for the static capacitance of some microstrip disk capacitors," *AEU*, band 39, vol. 4, pp. 269–272, 1985.

[5] T. Itoh and R. Mitra, "A new method for calculating the capacitance of a circular disk for microwave integrated circuits," *IEEE Trans. Microwave Theory Tech.*, vol. MTT-21, pp. 431–432, 1975.

[6] S. R. Borkar and R. F. Yang, "Capacitance of a circular disk for applications in microwave integrated circuits," *IEEE Trans. Microwave Theory Tech.*, vol. MTT-23, pp. 588–591, 1975.

[7] M. S Leong, P. S. Kooi, and K. P. Yeo, "Capacitance of a circular disc for applications in microwave integrated circuits," *IEE Proc.*, pt. H, vol. 128, no. 6, pp. 320–322, Dec. 1981.

[8] ——, "Determination of circular microstrip disc by Noble's variational method," *IEE Proc.*, vol. 128, pt. H, no. 6, pp. 306–104, 1980.

[9] W. Chew and J. A. Kong, "Effect of fringing fields on the capacitance of circular microstrip disk," *IEEE Trans. Microwave Theory Tech.*, vol. MTT-28, pp. 98–104, 1980.

[10] A. K. Sharma and W. J. R. Hoefer, "Spectral domain Analysis of a hexagonal microstrip resonator," *IEEE Trans. Microwave Theory Tech.*, vol. MTT-30, p. 825, 1982.

[11] M. S. Leong, P. S. Kooi, and A. L. Satya Prakash, "Finite element analysis of shielded microstrip disc resonator," *IEE Proc.*, pt. H, vol. 131, no. 2, pp. 126–128, Apr. 1984.

[12] B. Bhat and S. K. Koul, "Lumped capacitance, open circuit end effects, and edge-capacitance of microstrip like transmission lines for microwave and millimeter wave applications," *IEEE Trans. Microwave Theory Tech.*, vol. MTT-32, pp. 433–439, Apr. 1984.

[13] R. Crampagne, M. Ahmadpanah, and J. L. Guirand, "A Simple method for determining the Green's function for a large class of MIC lines having multilayered dielectric structures," *IEEE Trans. Microwave Theory Tech.*, vol. MTT-28, pp. 82–87, Feb. 1978.

[14] A. K. Verma and Z. Rostamy, "Modified Wolff model for the resonant frequency of covered rectangular microstrip patch antenna," *Electron. Lett.*, vol. 24, pp. 1850–1852, Sept. 1991.

[15] ——, "Modified Wolff model for the determination of resonant frequency of dielectric covered circular microstrip patch antenna," *Electron. Lett.*, vol. 24, pp. 2234–2236, Nov. 1991.

[16] K. F. Lee and J. S. Dahele, "Circular disc microstrip antenna with an airgap," *IEEE Trans. Antenn. Propagat.*, vol. AP-32, pp. 880–884, Aug. 1984.

[17] A. K. Verma, A. Bhaupal, Z. Rostamy, and G. P. Srivastava, "Analysis of rectangular patch antenna with dielectric cover," in *IEICE Trans.*, vol. E. 74, no. 5, pp. 1270–1279, May 1991.

[18] E. Yamashita, "Variational method for the analysis of microstrip like transmission lines," *IEEE Trans. Microwave Theory Tech.*, vol. MTT-16, pp. 529–535, Aug. 1068.

[19] G. Kompa and R. Mehran, "Planar waveguide model for calculating microstrip components," *Electron. Lett.*, vol. 11, no. 9, pp. 459–4460, 1975.

[20] P. Benedek and P. Silvester, "Capacitance of Parallel rectangular plates separated by a dielectric sheet," *IEEE Trans. Microwave Theory Tech.*, vol. MTT-20, pp. 504–510, Aug. 1972.

[21] A. Benalla and K. C. Gupta, "Multiport network model for rectangular microstrip patches covered with a dielectric layer," *IEE Proc.*, vol. 137, pp. 6, pp. 377–383, Dec. 1990.

[22] Z. Rostamy and A. K. Verma, "Resonant frequency of dielectric covered hexagonal patch," in *Int. Symp. Antenn. Propagat.* , Cohin, India, Dec. 1992.

[23] R. K. Hoffman, *Handbook of Microwave Integrated Circuit.* Norwood, MA: Artech House, 1987, pp. 149–150.

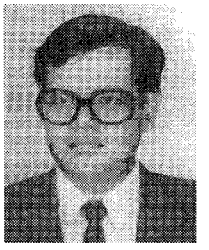

Anand K. Verma (M'92) was born on October 2, 1948. He received the B. Tech. degree in electronics and communication engineering from B.I.T. Sindri, India in 1970, and the Ph.D. degree in microwave engineering in 1983.

He has been associated with maintenance & installation of Radio & TV transmitters, antennas, and satellite communication systems. Presently, he is a reader with the Department of Electronic Science, University of Delhi, India. His present interest is in modeling, analysis and design of multilayers microstrip line patches and resonators for MMIC/MIC, antennas, filters, and pulse propagation.

He is a Fellow of IETE, India, and a Fellow of the Broadcast Society of India. He has chaired a session on microstrip antenna at APMC '90, Tokyo, Japan. He was secretary of National Symposium of Advances in Microwaves in 1993, New Delhi, India. He was also Secretary of the Exhibition Committee of ISRAMT '93, New Delhi, India.

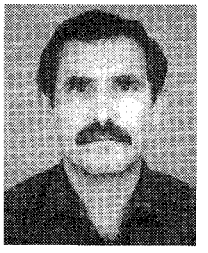

Zargham Rostamy was born in Khallkhal, Iran, in 1953. He received the M.Sc. degree in physics from the University of Meerut, India, in 1988. He received the Ph.D. degree in 1993 from Delhi University, South Campus, in microwaves.

Presently, he is with University of Imam Hussain, Tehran, Iran. His area of interest is in multilayered microstrip antennas and resonating structures.